Laboratory Investigation (2020) 100:1184–1196
https://doi.org/10.1038/s41374-020-0434-3

ARTICLE

Blocking thrombospondin-1 signaling via CD47 mitigates renal interstitial fibrosis

Sohel M. Julovi[1] · Barkha Sanganeria[1] · Nikita Minhas[1] · Kedar Ghimire[1] · Brian Nankivell[1,2,3] · Natasha M. Rogers[1,2,3,4]

Received: 18 January 2020 / Revised: 31 March 2020 / Accepted: 11 April 2020 / Published online: 4 May 2020

Abstract

Acute kidney injury triggers a complex cascade of molecular responses that can culminate in maladaptive repair and fibrosis. We have previously reported that the matrix protein thrombospondin-1 (TSP1), binding its high affinity its receptor CD47, promotes acute kidney injury. However, the role of this pathway in promoting fibrosis is less clear. Hypothesizing that limiting TSP1–CD47 signaling is protective against fibrosis, we interrogated this pathway in a mouse model of chronic ischemic kidney injury. Plasma and renal parenchymal expression of TSP1 in patients with chronic kidney disease was also assessed. We found that $CD47^{-/-}$ mice or wild-type mice treated with a CD47 blocking antibody showed clear amelioration of fibrotic histological changes compared to control animals. Wild-type mice showed upregulated TSP1 and pro-fibrotic markers which were significantly abrogated in $CD47^{-/-}$ and antibody-treated cohorts. Renal tubular epithelial cells isolated from WT mice showed robust upregulation of pro-fibrotic markers following hypoxic stress or exogenous TSP1, which was mitigated in $CD47^{-/-}$ cells. Patient sera showed a proportionate correlation between TSP1 levels and worsening glomerular filtration rate. Immunohistochemistry of human kidney tissue demonstrated tubular and glomerular matrix localization of TSP1 expression in patients with CKD. These data suggest that renal tubular epithelial cells contribute to fibrosis by activating TSP1–CD47 signaling, and point to CD47 as a potential target to limit fibrosis following ischemic injury.

Introduction

Chronic kidney disease (CKD) is a global public health burden, affecting ~10% of the population worldwide regardless of socioeconomic status [1]. The underlying cause of renal damage can vary extensively, from immunological to surgical to iatrogenic injury. However, the final common pathway of cellular repair establishes a maladaptive process culminating in excessive connective tissue deposition and disruption of functioning nephron units [2]. Robust epidemiological evidence demonstrates that patients surviving acute kidney injury (AKI) recover incompletely, with persistent hemodynamic and hypoxic changes within the renal parenchyma despite normal serum creatinine [3]. The burgeoning fibrotic matrix contributes to rarefaction of the crucial peri-tubular capillary network [4], leading to diminished renal parenchymal perfusion that manifests as loss of kidney volume.

The major cellular events leading to the development of fibrosis, and thus CKD, are diverse and are not instigated by a single cell population. The inflammatory response, activation and accumulation of myofibroblasts, and uncontrolled renal tubular epithelial cell (RTEC) damage all contribute to the fibrotic process. Early studies of CKD found an inverse correlation between tubular epithelial cell area and degree of interstitial fibrosis [5, 6]. Experimental evidence has established that RTEC injury leads to modifications favoring a mesenchymal phenotype, G2/M

These authors contributed equally: Sohel M. Julovi, Barkha Sanganeria

✉ Natasha M. Rogers
natasha.rogers@health.nsw.gov.au

[1] Centre for Transplant and Renal Research, Westmead Institute for Medical Research, Camperdown, NSW, Australia

[2] Westmead Clinical Medical School, University of Sydney, Camperdown, NSW, Australia

[3] Renal Division, Westmead Hospital, Camperdown, NSW, Australia

[4] Department of Surgery, Thomas E. Starzl Transplantation Institute, University of Pittsburgh School of Medicine, Pittsburgh, PA, USA

cell cycle arrest and subsequent elaboration of fibrogenic factors [7]. This widely accepted paradigm of epithelial–mesenchymal transition (EMT) is characterized by loss of epithelial proteins such as cytokeratin, and acquisition of markers including vimentin and α-smooth muscle actin [8].

TSP1 is a 450 kDa protein that forms a component of the matrix scaffold. However, rather than providing structural integrity, TSP1 modulates cell function as well as the function of protein, growth factors and enzymes. Many cell types secrete TSP1 in response to stress, including RTEC [9]. TSP1 possesses multiple binding domains that allow interactions with numerous ligands and receptors (comprehensively reviewed in ref. [10]), including β-integrins, CD36, SIRP-α and CD47 [11]. Experimental evidence favors CD47, the universally expressed integral membrane protein, as the high affinity and necessary receptor for most TSP1-mediated cell responses [12]. TSP1 is also a regulator of the major profibrotic cytokine, transforming growth factor (TGF)-β, suggesting that TSP1 may drive the synthesis and accumulation of matrix. Indeed, TSP1 and TGF-β transcriptional activity is linked in mesangial cells [13], and TSP1null mice demonstrate attenuation of diabetic glomerular changes [14] or crescent formation in anti-glomerular basement membrane disease [15]. No studies to date have examined the role of TSP1 in RTEC and their contribution to fibrosis in mouse models or human disease.

We have previously published that TSP1 and CD47 are upregulated in acute kidney injury [9]. Here we describe an important role for both TSP1 and CD47 in promoting chronic renal injury and fibrosis, and stimulating RTEC-based production of fibrogenic factors. For the first time, we demonstrate that plasma TSP1 is upregulated in patients with a significant renal impairment, and that TSP1 is detectable in the RTEC and glomerular matrix in diseased human kidneys, regardless of etiology.

Materials and methods

Reagents and cells

Human renal tubular epithelial cells (RTEC) were purchased from Lonza (Basel, Switzerland) and maintained in recommended medium. Cells from passage 2–6 were used for experimental work. Antibodies against α-smooth muscle actin (SMA) (clone EPR5368), vimentin (clone EPR3776), transforming growth factor (TGF)-β (ab92486), vinculin (clone EPR8185) and SMAD2 (clone EP567Y) and TSP1 (clone A6.1) were from Abcam (Cambridge, UK). Antibodies against β-actin (clone 8H10D10) were from Cell Signalling Technologies (Danvers, MA). Anti-CD47 antibodies (mouse clone MIAP301, human clone B6H12), CTGF (clone B6) as well as isotype control antibodies (rat anti-mouse IgG) were from Santa Cruz Biotechnology (Dallas, TX). Recombinant thrombospondin-1 was sourced from Athens Research & Technology (Athens, GA).

Animals

$CD47^{-/-}$ (#003173) mice were from The Jackson Laboratory (Bar Harbor, ME). As per the provider, $CD47^{-/-}$ ($B6.129S7\text{-}^{Cd47tm1Fpl/J}$) mice were backcrossed at least 15 times into the C57BL/6 background. A separate colony of $CD47^{-/-}$ mice was maintained at Australian BioResources (ABR, Sydney, Australia). C57BL/6 mice were also from ABR. All studies were performed using protocols approved by the Western Sydney Local Health District Animal Ethics Committee (#5128) and performed in accordance with the Australian code for the care and use of animals for scientific purposes developed by the National Health and Medical Research Council of Australia.

Renal injury models

Age-matched male mice were anaesthetized using isoflurane and body temperature maintained at 36 °C. For the ischemia–reperfusion–nephrectomy (IR-N) model, a microvascular clamp occluded the left renal pedicle for 22 min. The abdomen was closed with 5/0 monofilament. The contralateral kidney was removed at day (D) + 7 and mice were subsequently sacrificed at D + 28. In additional experiments, anti-CD47 antibody (αCD47Ab or isotype control IgG) was administered to WT mice via intraperitoneal injection (0.8μg/g body weight) 1 week after renal IR and continued weekly until killing.

Kidney histology

Kidneys embedded in paraffin were sectioned at 4 μm and stained with hematoxylin and eosin using standard methods [16]. Picosirius red staining was also performed according to standard protocol. Sections were deparaffinized and placed in a 0.1% solution of Sirius in picric acid for 4 h in the dark, washed and coverslipped with mounting media. Slides were viewed under brightfield conditions. Fibrosis scores were assessed in five randomly selected corticomedullary areas and quantified using ImageJ as published previously [17]. The amount and intensity of staining was calculated by initially setting a threshold and measuring within regions of interest. All slides were analyzed simultaneously with identical software settings.

Assessment of renal function

Renal function was determined by measurement of serum creatinine using the Siemens Dimension Vista® System.

Murine RTEC cultures

Primary wild-type (WT) and $CD47^{-/-}$ cells were harvested as described previously [18]. Kidneys were digested using multi-tissue dissociation kit and GentleMacs (Miltenyi, Bergisch Gladbach, Germany), incubated with CD326 (EpCAM) microbeads (Miltenyi) and passed through LS columns. The positive cell fraction was suspended in defined K1 medium: DMEM/F12 medium supplemented with 25 ng/ml epidermal growth factor (Sigma-Aldrich, St Louis, MO), 1 ng/ml prostaglandin E_1 (Cayman Chemicals, Ann Arbor, MI), 5×10^{-11} M triiodothyronine (Sigma-Aldrich), 5×10^{-8} M hydrocortisone (Sigma-Aldrich), insulin–transferrin–sodium selenite supplement (Sigma-Aldrich), 1% penicillin/streptomycin (ThermoFisher Scientific, Waltham, MA), 25 mM HEPES (ThermoFisher Scientific), and 5% FCS (ThermoFisher Scientific), and cultured on collagen-coated dishes (BD Biosciences, Franklin Lakes, NJ).

Cell passages 2–4 were used for experimental work. In certain experiments, cells were cultured in serum-starved media (0.5% FCS) and subjected to normoxia (FiO_2 21%), hypoxia (FiO_2 1%) and exogenous TSP1 (2.2 nM) with or without CD47 antibody (1 µg/ml) for 24 h.

Western blot analysis

Tissue or cells were homogenized in cold RIPA buffer (Cell Signaling Technology) that contained protease inhibitor cocktail (Sigma-Aldrich) and phosphatase inhibitor cocktail (Roche Applied Science, Hercules, CA). Lysates were quantified using a DC™ assay (BioRad, Hercules, CA). Protein was resolved by SDS-PAGE and transferred onto nitrocellulose membranes (BioRad). Blots were probed with primary antibodies and visualized on an Odyssey Imaging System (Licor, Lincoln, NE) using ImageStudioLite (Licor). The intensity of the bands was quantified using ImageStudioLite.

RNA extraction and quantification by real-time PCR

RNA was extracted using ISOLATE-II RNA MiniKits (Bioline, London, UK) with on-column DNase treatment. RNA was quantified using a Nanodrop (BioTek, Winooski, VT), and reverse-transcribed using a SensiFAST cDNA synthesis kit (Bioline). cDNA was amplified in triplicate with gene-specific primers (Invitrogen) using a CFX384 real-time PCR machine (Biorad). Thermal cycling conditions were 95 °C for 2 min, followed by 40 cycles of 95 °C for 5 s and 60 °C for 30 s. Expression was normalized to the housekeeping gene and data were analyzed using the ΔΔCt method. WT sham-operated animals, untreated WT RTEC or untreated human RTEC were used as the referent controls to determine fold change in transcript in comparator groups.

Immunofluorescence

Cells were grown on glass bottom dishes (MatTek, Ashland, MA) and TSP1 (2.2 nM) was added for 24 h. Permeabilization was performed with PBS/10% BSA/0.1% Triton-X100 for 10 min at room temperature followed by blocking with 1% goat serum (Sigma-Aldrich) for 30 min. Cells were incubated in primary antibody (1:100 dilution) in blocking buffer in a humidified chamber at 4 °C overnight. Cells were washed then incubated with AF488 secondary antibody (1:400 dilution, Invitrogen) for 1 h. Nuclei were stained with DAPI. Cells were coverslipped with Gelvatol mounting media. Images were captured with an Olympus Fluoview 1000 confocal microscope, and results calculated as the percentage of area stained using ImageJ.

Plasma TSP1 measurement

The study was approved by the Human Research Ethics Committee of Western Sydney Local Health District [HREC LNR/12/WMEAD/114 and LNRSSA/12/WMEAD/117 (3503)]. All subjects provided written consent. Patients ($n = 108$) with varying estimated glomerular filtration rate (eGFR, determined by CKD-EPI) were recruited from outpatient clinics, and did not have an intercurrent illness or acute kidney injury. Blood was collected in EDTA tubes without a tourniquet using a 23-gauge needle, and placed immediately on ice. Platelet-poor plasma was generated by centrifugation at 2500 rpm for 15 min at 4 °C without brake, then stored at −80 °C until analysis. Plasma TSP1 concentration was determined by ELISA (Abcam). For the linear regression analysis, patients with no known renal disease and normal renal function were assumed to have GFR 90 ml/min, and dialysis-dependent patients had a GFR of 5 ml/min.

Immunohistochemistry

Two µm sections of paraffin-embedded human kidney biopsies were incubated with rabbit anti-thrombospondin-1 (TSP1) (Abcam, ab85762, 1 µg/ml), or isotype-matched IgG. For immunodetection, Dako EnVision+ System-HRP labeled polymer detection kit (Dako, Carpinteria, CA, USA) was used with ImmPACT NovaRED Peroxidase (HRP) Substrate (Vector Laboratories, Burlingame, CA), and counterstained by Mayer's hematoxylin and Scott's bluing solution. After mounting, slides were viewed by

NanoZoomer (Hamamatsu, Iwata City, Japan). All samples were stained in a single assay to exclude between-run variability.

Statistical analysis

Statistical analyses were performed using GraphPad Prism software. Data were analyzed by Student's *t*-test, Mann–Whitney *U*-test or ANOVA for multiple group comparisons. A Tukey's or Dunnett's multiple comparison post-test was performed where relevant. Linear regression analysis was used to determine the relationship between plasma TSP1 and eGFR. A p-value of < 0.05 was assumed to be significant.

Results

Absent CD47 and blockade of CD47 signaling is protective in an ischemic model of renal fibrosis

Employing a clinically relevant model of CKD, we performed unilateral ischemia–reperfusion (IR) injury followed by contralateral nephrectomy (denoted IR-N), reducing renal mass and subsequently relying upon a single injured kidney. WT kidney tissue sections demonstrated areas of impaired repair with thinned renal tubular epithelium which was not seen in CD47$^{-/-}$ mice (Fig. 1a). This pattern was further highlighted by Sirius Red staining (Fig. 1b, c). CD47$^{-/-}$ mice are resistant to acute injury in multiple models [9, 19, 20], and it is possible that subsequent protection from chronic injury was due to the initial resistance to parenchymal damage. It is difficult to accurately titrate a primary ischemic event to induce similar injury in WT and CD47$^{-/-}$ kidneys, therefore we subjected WT mice to IR-N and administered αCD47 or isotype control antibody (Ab) 1 week following injury (at the time of nephrectomy). This ensured consistency between ischemic events, and that the subsequent mitigation of chronic injury alone was due to limiting TSP1–CD47 signaling. Administration of αCD47Ab, but not isotype control antibody, significantly improved histology and fibrosis, similar to that seen in CD47$^{-/-}$ mice (Fig. 1c). Serum creatinine was not significantly different between groups (Fig. 1d).

Intact TSP1–CD47 signaling promotes expression of fibrotic markers

To determine whether CD47$^{-/-}$ or αCD47Ab-treated kidneys demonstrated a reduction in fibrotic markers consistent with histology improvements, we evaluated protein and transcript expression. TSP1 protein was indeed elevated in the context of chronic injury in WT mice (Fig. 2a), but was mitigated in CD47$^{-/-}$ and αCD47Ab-treated IR-N mice. TSP1 has been shown to activate latent TGF-β [21, 22]. The pattern of TGF-β expression in whole kidneys closely followed that of TSP1: expression of TGF-β was lowest in sham-operated animals and greatest in WT mice, with mitigated expression in both CD47$^{-/-}$ and αCD47Ab-treated mice (Fig. 2b). The low molecular weight of TGF-β (14 kDa) is difficult to resolve adequately and to confirm our results, we assessed a downstream effector molecular crucial to TGF-β signal transduction, SMAD2, which was down-regulated in CD47$^{-/-}$ and αCD47Ab-treated IR-N mice (Fig. 2c). Connective tissue growth factor (CTGF) is similar to TSP1 as a secreted matricellular protein that can modulate cell signaling pathways and promote matrix deposition and remodeling [23]. CTGF expression was elevated in WT IR-N and mitigated in both CD47$^{-/-}$ mice and antibody-treated WT mice (Fig. 2d). Expression of α-smooth muscle actin (αSMA) is indicative of activated fibroblasts, which have a high synthetic capacity for extracellular matrix proteins. Damaged RTEC demonstrate a phenotypic change characterized by de novo synthesis of αSMA [24]. Upregulation of αSMA transcript was greatest in WT IR-N mice (Fig. 2e). Expression of vimentin was constitutively upregulated regardless of the presence of TSP1–CD47 signaling (Fig. 2f).

Fibrotic kidneys and renal tubular epithelial cells (RTEC) elaborate matrix, which is mitigated by absent CD47

To assess any correlation between whole kidney protein and transcript expression, we analyzed mRNA expression of multiple fibrotic markers (Fig. 3). TSP1 mRNA was elevated in WT IR-N mice, but expression was reduced in CD47$^{-/-}$ and αCD47Ab-treated animals. The pattern of TGF-β transcript expression replicated that of TSP1. Upregulation of αSMA transcript was greatest in WT IR-N mice. Type I collagen and fibronectin were similarly upregulated in WT mice but mitigated by blockade or absence of CD47 signaling.

RTEC are the dominant renal parenchymal cell and contribute to synthesis and secretion of matrix through epithelial-to-mesenchyme transition (EMT) [25, 26]. To interrogate alterations in RTEC-based matrix production, we isolated WT and CD47$^{-/-}$ cells, subjected them to 24 h normoxia or hypoxia (FiO_2 1%) and assessed mRNA expression of TSP1 and fibrotic markers (Fig. 4a). TSP1 transcript was substantially upregulated in WT RTEC compared to CD47$^{-/-}$ cells following hypoxic exposure. Only hypoxic WT RTEC consistently upregulated αSMA, type I collagen, and fibronectin transcript compared to both normoxic WT and CD47$^{-/-}$ cells. TGF-β mRNA expression was significantly increased in WT cells in response to hypoxia compared to CD47$^{-/-}$ RTEC.

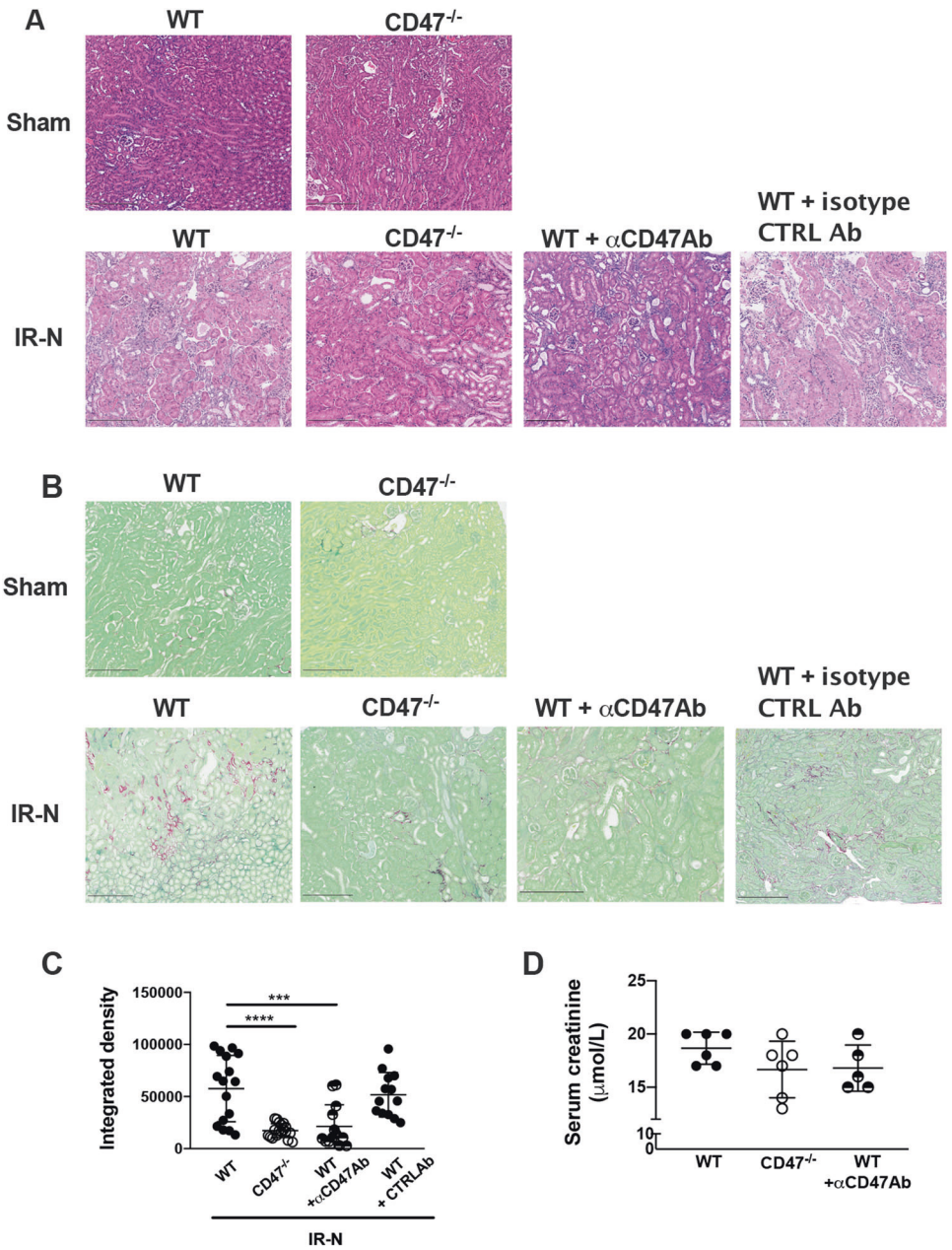

Fig. 1 Absent CD47 protects against the development of renal fibrosis. Age-matched male WT and CD47$^{-/-}$ mice, as well as WT mice receiving αCD47 or isotype control antIbody were subjected to unilateral renal ischemia–reperfusion injury + contralateral nephrectomy (IR-N). At D + 28 post-IR-N, kidney tissues were sectioned and stained with **a** hematoxylin and eosin (H&E) or **b** Sirius red, followed by **c** quantitative analysis of fibrosis. **d** Serum creatinine was measured. All data are presented as mean ± SD from $n = 6$–8 samples; $^{**}p < 0.01$, $^{***}p < 0.001$, $^{****}p < 0.0001$. Representative photomicrographs are shown, original magnification ×10, scale bar is 250 μm.

The TSP1 gene contains a hypoxia response element [27], and while hypoxia is a useful surrogate to examine cell responses, it lacks specificity. To explicitly examine the role of TSP1 on RTEC and the elaboration of fibrosis markers, we added TSP1 at 2.2 nM to WT or CD47$^{-/-}$ cells and then performed immunofluorescent staining for TGF-β. Exogenous TSP1 at this concentration will only engage CD47 [12]. TSP1 at 2.2 nM significantly increased TGF-β expression in WT cells, and this response was mitigated in the absence of CD47 (Fig. 4b). Exogenous TSP1 also induced markers of fibrosis, including αSMA, type I collagen and fibronectin (Fig. 4c). mRNA levels of TSP1, TGF-β, type I collagen, and fibronectin in response to TSP1 was significantly suppressed in CD47$^{-/-}$ RTEC compared to WT cells. The addition of αCD47Ab to WT cells downregulated TSP1 and αSMA transcript, but otherwise there was no substantial effect on fibrotic markers in WT cells, unlike that seen in vivo. We have previously seen differences in effects mediated by CD47 blocking antibody, with minimal responses in vitro in contrast with an in vivo response, as well as differences in the efficacy of antibody clones to change signal transduction. [16]

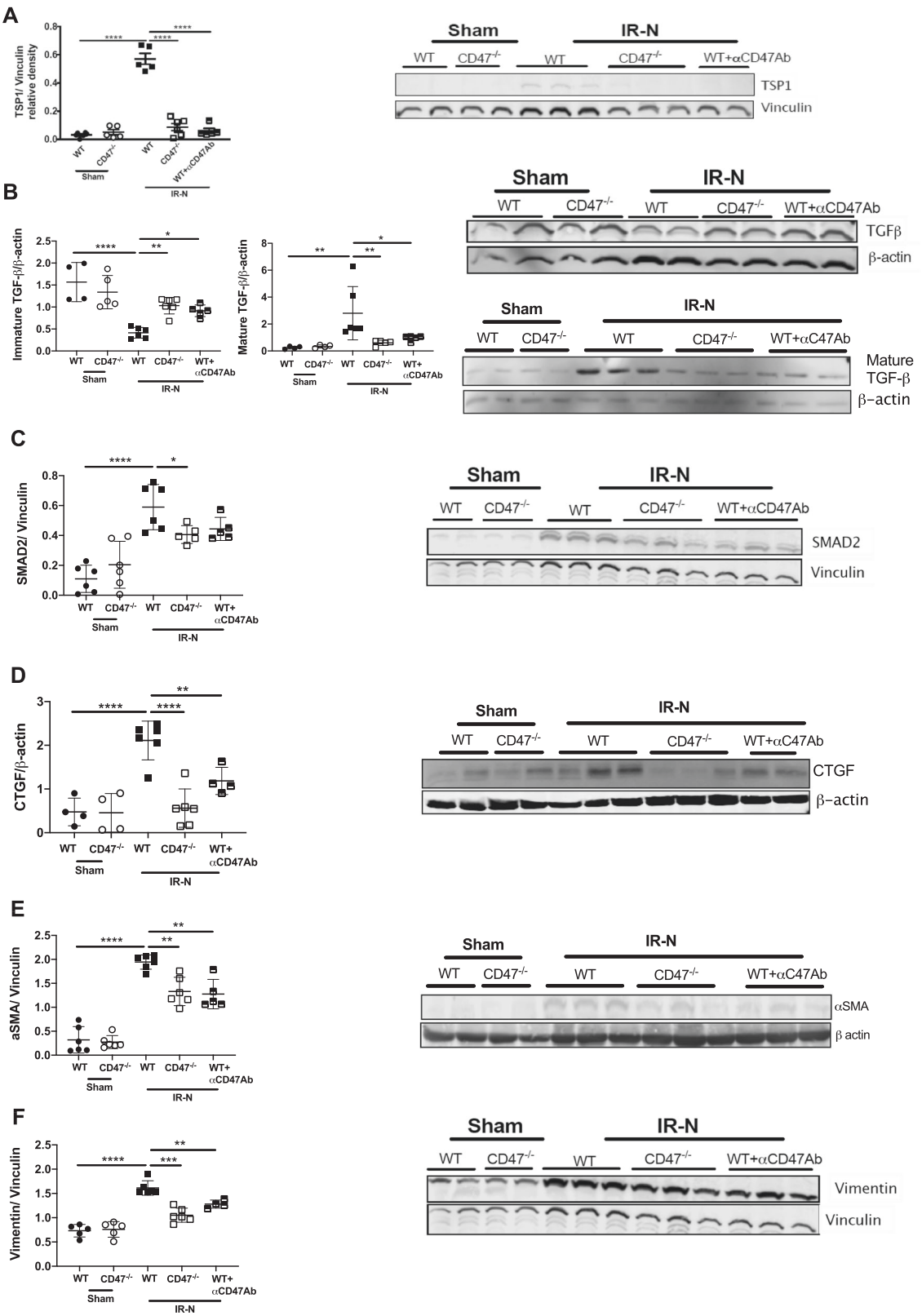

Fig. 2 TSP1–CD47 signaling promotes epithelial–mesenchymal transition and elaboration of matrix in renal fibrosis. Whole kidney homogenate from WT and CD47$^{-/-}$ mice, as well as WT mice receiving αCD47Ab was resolved by SDS-PAGE for fibrotic markers. Quantification of protein expression, in addition to representative western blots for **a** thrombospondin-1 (TSP1), **b** α-smooth muscle actin (αSMA), **c** transforming growth factor (TGF)-β, **d** connective tissue growth factor (CTGF), **e** SMAD2 and **f** vimentin. Densitometry is presented as the mean ratio of target protein to loading control (β-actin or vinculin) ± SD from $n = 3–8$ samples. *$p < 0.05$, **$p < 0.01$, ***$p < 0.001$, ****$p < 0.0001$.

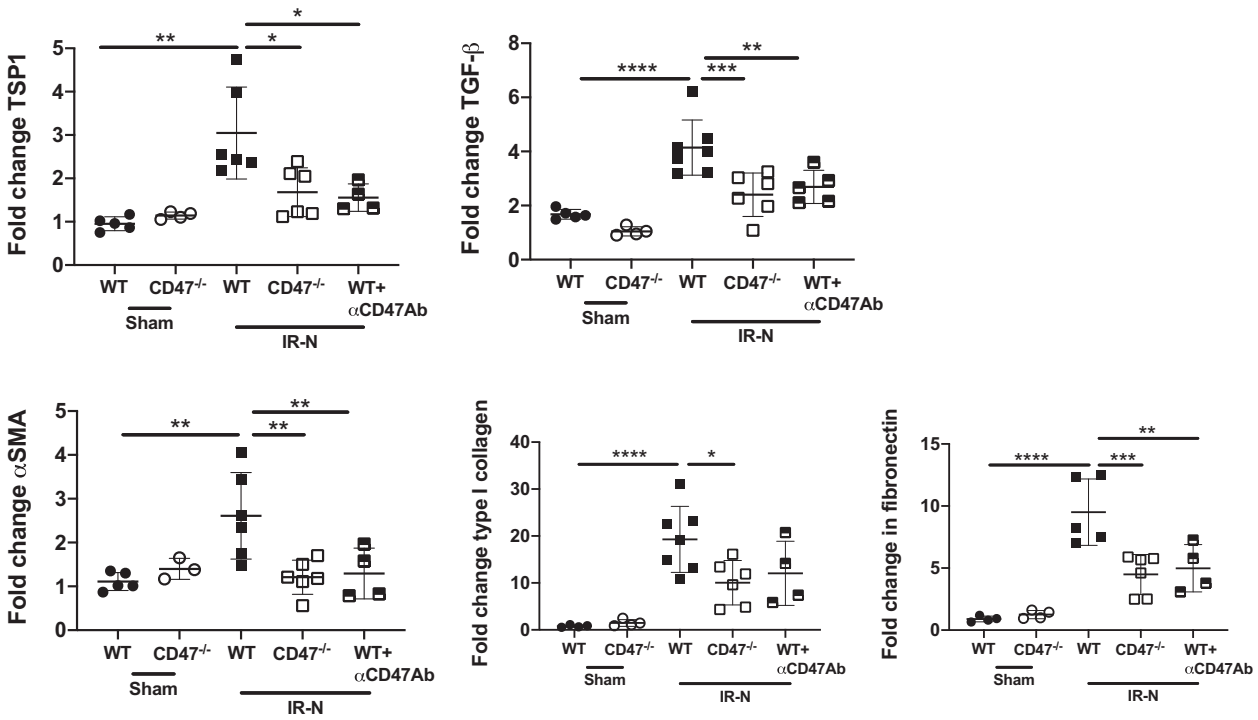

Fig. 3 Limiting TSP1–CD47 in the renal parenchyma reduces matrix in chronic kidney injury. Whole kidney homogenate from WT and CD47$^{-/-}$ IR-N, as well as WT mice receiving αCD47Ab was prepared for qPCR analysis. All samples were collected for RNA isolation, cDNA synthesis and RT-PCR performed for TSP1, αSMA, type I collagen, fibronectin and TGF-β. PCR was run in triplicate and results are presented as fold change ± SD from $n = 3$–6 independent experiments, *$p < 0.05$, **$p < 0.01$, ***$p < 0.001$, ****$p < 0.0001$.

Plasma TSP1 is elevated in CKD

TSP1 has been shown to be elevated in plasma of patients with pulmonary hypertension [28] and peripheral vascular disease [29]. A relationship between plasma TSP1 and CKD, specifically glomerular filtration rate, has never been demonstrated. We measured platelet-poor plasma TSP1 concentrations in patients with normal renal function and CKD (stages I–V), including end-stage kidney disease. Stage of CKD was determined by serum creatinine and therefore estimated glomerular filtration rate (eGFR) calculated according to the CKD-EPI equation [30]. We demonstrated a significant rise in plasma TSP1 as CKD progressed, particularly to stage IV and V (Fig. 5a). Linear regression analysis demonstrated a significant negative relationship between eGFR and plasma TSP1 ($r^2 = 0.2699$, $p < 0.0001$). Demographic characteristics of patients and the range of plasma TSP1 concentrations are found in Table 1.

Human renal tubular epithelial cells (RTEC) elaborate matrix which is mitigated by limiting CD47 signaling

We have previously published differences in responsiveness between mouse and human RTEC [16]. We therefore tested the response of human RTEC to exogenous TSP1 in the context of CD47 blockade. All fibrotic markers were induced with TSP1, and mitigated by αCD47Ab (Fig. 5b). Hypoxia alone was an insufficient stimulus to alter mRNA expression of any markers (data not shown). De novo expression of αSMA, the hallmark of EMT, was demonstrated in human RTEC incubated with 2.2 nM TSP1 (Fig. 5c).

TSP1 is expressed in human kidneys with CKD

Having demonstrated the presence of TSP1 transcript and protein expression in the kidneys of mice with chronic injury (Figs. 2, 3), elevated plasma TSP1 in patients with CKD, and the induction of fibrotic markers in human RTEC in response to TSP1, we performed immunohistochemical staining for TSP1 on human kidney biopsies. Patients with thin membrane disease (normal serum creatinine, microscopic hematuria, $n = 3$) were used as controls, and compared to patients with CKD grouped according to the presence of type II diabetes as a comorbidity (yes: $n = 9$; no: $n = 8$). Patient demographics are described in Table 2. In control kidneys, TSP1 staining was absent from glomeruli and present at low levels within the renal tubules (Fig. 5d(i)). Glomerular, punctate tubular epithelial, and peri-tubular TSP1 expression was only mildly increased in

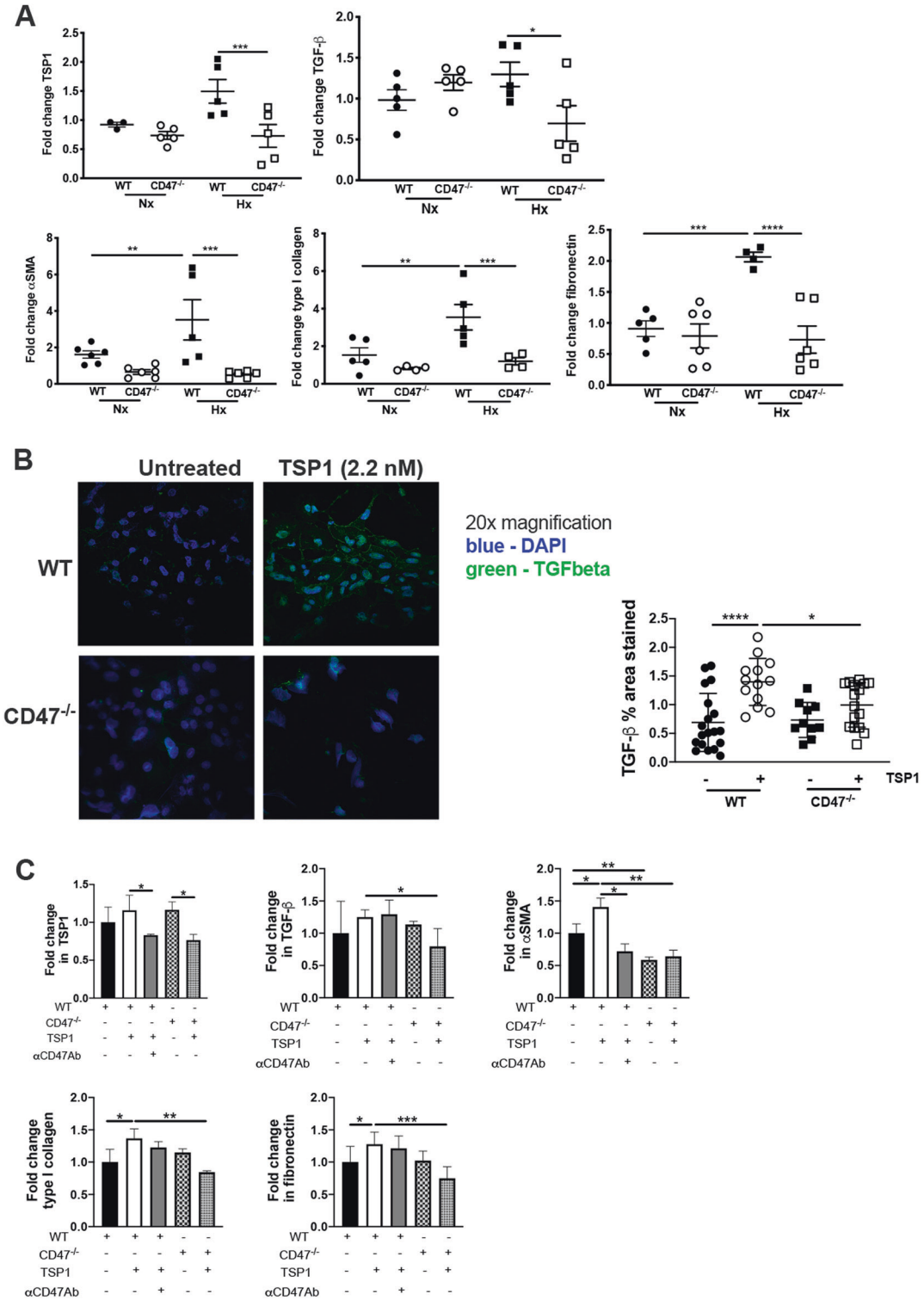

Fig. 4 WT, but not CD47$^{-/-}$ renal tubular epithelial cells (RTEC) significantly contribute to matrix production and epithelia-to-mesenchyme transition. WT and CD47$^{-/-}$ RTEC were isolated, grown to 70% confluence and exposed to serum-starved media. **a** Cells were exposed to serum-starved media plus normoxia (Nx, FiO_2 21%) or hypoxia (Hx, FiO_2 1%) for 24 h. All samples were collected for RNA isolation, cDNA synthesis and RT-PCR performed for TSP1, αSMA, type I collagen, fibronectin and TGF-β. **b** RTEC were treated with exogenous TSP1 (2.2 nM) for 24 h, stained for TGF-β (green) and DAPI (blue) and visualized by immunofluorescence. Representative photomicrographs at ×20 magnification are shown. The total cellular area stained was calculated from six randomly chosen regions of interest, from $n = 3$ independent experiments. **c** RTEC were treated with exogenous TSP1 (2.2 nM) for 24 h, with/without αCD47Ab (1 μg/ml). RT-PCR performed for TSP1, TGF-β, type I collagen, fibronectin and αSMA. All qPCR was run in triplicate and results are presented as fold change ± SD from $n = 4$–6 independent experiments, $^{*}p < 0.05$, $^{**}p < 0.01$, $^{***}p < 0.001$, $^{****}p < 0.0001$.

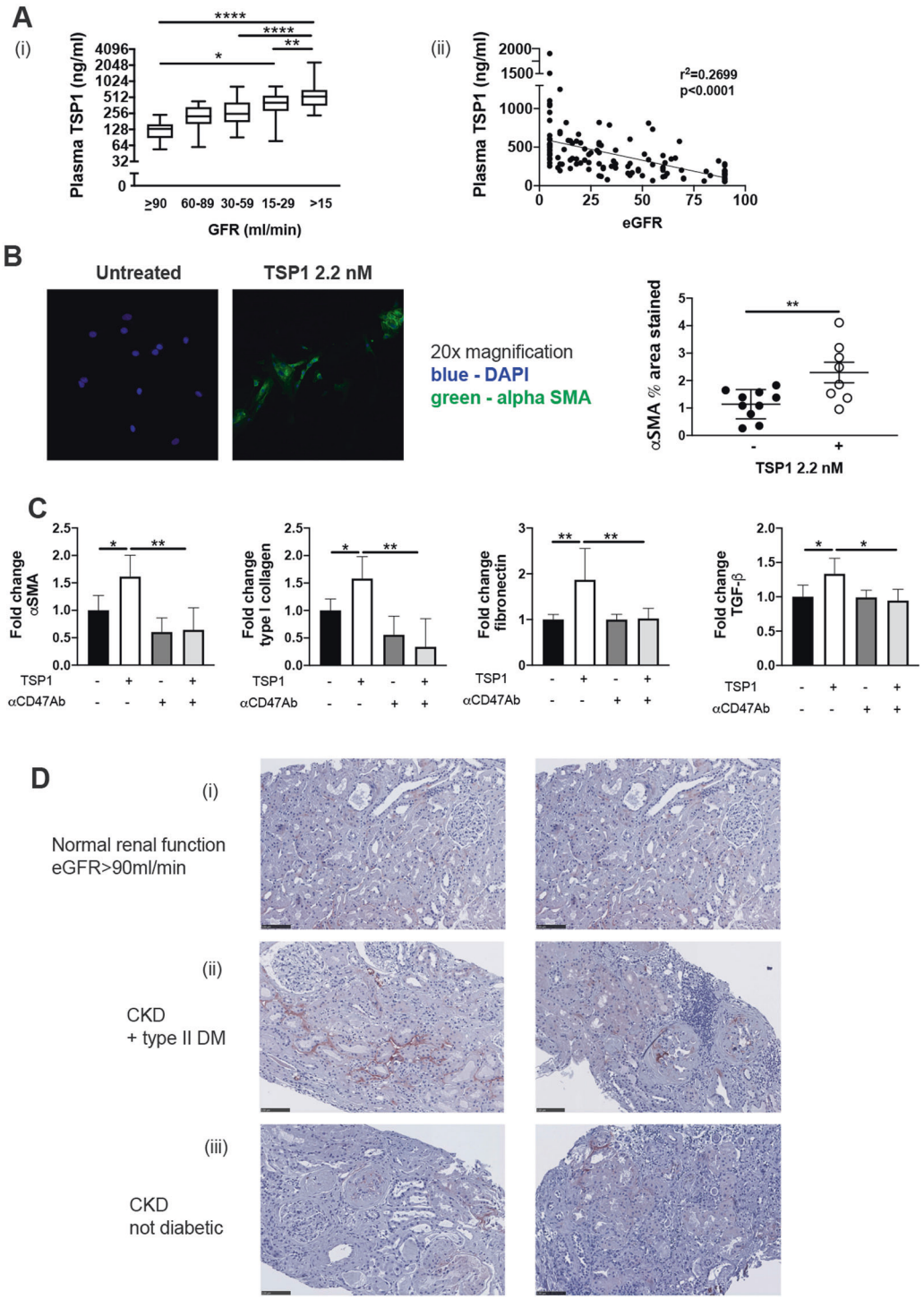

Fig. 5 TSP1 plasma levels are increased and tissue expression is enhanced in patients with chronic kidney disease. a Platelet-poor plasma was collected and TSP1 levels measured by ELISA. Results are graphed by (i) stage of CKD, and displayed as mean ± SD, with box and whisker plot displaying minimum and maximum values and (ii) linear regression analysis. **b** Human RTEC were grown to 70% confluence and treated with serum-starved media. Cells were exposed to exogenous TSP1 (2.2 nM) for 24 h, fixed, stained for αSMA and assessed by immunofluorescence. Representative photomicrographs at ×20 magnification are shown. The total cellular area stained was calculated from three randomly chosen regions of interest, from $n = 3$ independent experiments. **c** Human RTEC were exposed to exogenous TSP1 (2.2 nM) for 24 h, with/without αCD47Ab (1 μg/ml). RNA was extracted from cell lysates, converted to cDNA and RT-PCR performed for TSP1, TGF-β, type I collagen, fibronectin and αSMA. All qPCR was run in triplicate and results are presented as fold change ± SD from $n = 4$–6 independent experiments; $^{*}p < 0.05$, $^{**}p < 0.01$, $^{****}p < 0.0001$. **d** Immunohistochemical staining of TSP1 in (i) normal kidneys, (ii) diseased kidneys with type II diabetes mellitus as a comorbidity, and (iii) diseased kidneys without type II diabetes mellitus. Representative photomicrographs of $n = 2$ patients from each group are demonstrated at ×20 magnification, scale bar is 100 μm.

Table 1 Demographic characteristics and comorbidities of patients with measured plasma TSP1.

eGFR (ml/min)	≥90	60–89	30–59	15–29	<15	*p*-value[a]
N	13	13	24	23	35	
Age ± SD	42.2 ± 13.2	60.6 ± 20.9	68 ± 18.8	64.1 ± 17.7	67.1 ± 10.6	$p < 0.0001$
Female: male	10:3	8:5	10:14	11:12	16:19	NS
Type II diabetes, *N* (%)	0 (0)	5 (38.5)	14 (58.3)	13(60.9)	24 (68.6)	$p < 0.01$
Ischemic heart disease, *N* (%)	0 (0)	3 (23.1)	5 (20.8)	6 (23)	21 (60)	$p < 0.001$
Hypertension, *N* (%)	0 (0)	4 (30.8)	19 (79.2)	14 (60.9)	28 (80)	$p < 0.0001$
Peripheral vascular disease, *N* (%)	0 (0)	1 (7.7)	7 (29.2)	2 (9.5)	7 (20)	NS
Plasma TSP1 mean concentration ± SEM (ng/ml)	128.7 ± 14.6	237.4 ± 30.1	328.8 ± 43.5	405.6 ± 36.3	630 ± 70.3	$p < 0.0001$
Minimum plasma TSP1 (μg/ml)	54.1	59.8	90.5	77.2	234.4	
Maximum plasma TSP1 (μg/ml)	240.2	431.3	810.8	820.5	2300	

[a]Ordinary one-way ANOVA; Tukey multiple comparison test is shown in Fig. 5a panel (i).

Table 2 Demographic characteristics of human biopsies analyzed for TSP1 expression.

Patient no.	Gender	Age (y)	Serum creatinine (μmol/l); eGFR (ml/min) at biopsy	Co-morbid conditions	Proteinuria (g), hematuria	Diagnosis
1	M	60	170; 40	HT	3, Y	FSGS, interstitial fibrosis
2	F	34	90; >90	nil	4.5, N	MCGN, 10% interstitial fibrosis
3	M	70	195; 31	Type II DM (T2DM)	6.3, N	FSGS, 30% interstitial fibrosis
4	M	79	195; 41	HT	2.5, N	FSGS, 30% interstitial fibrosis
5	M	66	90; 80	HT, T2DM	2.4, N	FSGS, 40% interstitial fibrosis
6	M	51	90; >90	nil	Nil, Y	Thin membrane disease
7	M	53	330; 23	HT, T2DM	6.8 g, N	Diabetic nephropathy, 60% interstitial fibrosis
8	F	49	80; >90	nil	Nil, Y	Thin membrane disease
9	M	70	215; 28	HT, T2DM	Nil, N	Hypertensive glomerulosclerosis, 30% interstitial fibrosis
10	M	49	400; 20	T2DM	4, N	Diabetic nephropathy, 70% interstitial fibrosis
11	M	62	100; 83	HT, smoker	0.5, Y	50% chronic interstitial fibrosis
12	F	50	160; 40	HT	0.4, N	30% interstitial fibrosis
13	M	65	115; 60	T2DM	2.8, N	Diabetic nephropathy
14	M	71	200; 38	Nil	0.84, N	FSGS, 50% interstitial fibrosis
15	M	72	100; 73	HT	3.3, Y	FSGS, 15% interstitial fibrosis
16	M	78	250; 24	HT	3.5, N	FSGS, 50% interstitial fibrosis
17	F	68	215; 25	HT, T2DM	1.0, N	Diabetic nephropathy, 60% interstitial fibrosis
18	M	56	260; 30	T2DM	Nil, N	Diabetic nephropathy, 40% interstitial fibrosis
19	M	59	185; 48	HT, T2DM	0.35, N	MCGN, 60% interstitial fibrosis
20	F	52	80; >90	Nil	Nil, Y	Thin membrane disease

HT hypertension, *type II DM (T2DM)* type 2 diabetes mellitus, *MCGN* mesangiocapillary glomerulonephritis, *FSGS* focal segmental glomerulosclerosis.

patients with CKD regardless of the presence of diabetes (Fig. 5d(ii), (iii)). TSP1 staining was localized and sufficiently low throughout all sections to prevent accurate measurements of staining intensity.

Discussion

CKD is one of the most challenging chronic disorders affecting the Western world [31]. Excessive matrix

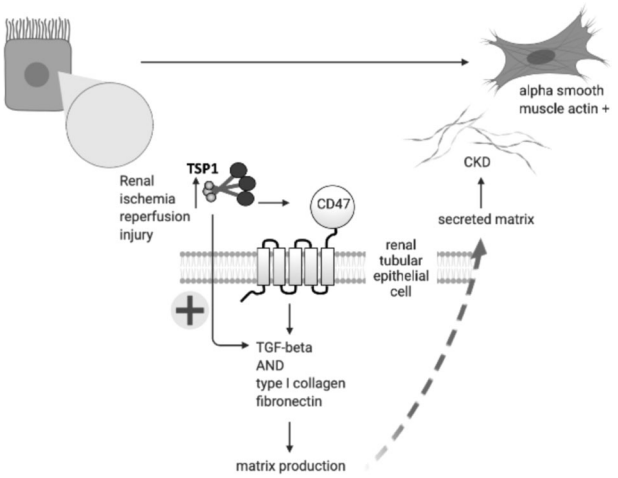

Fig. 6 TSP1 via CD47 on renal tubular epithelial cells induces production matrix proteins to promote fibrosis. TSP1 is produced by renal tubular epithelial cells (RTEC) in response to stress, such as ischemic/hypoxic injury, and binds to CD47 to produce fibrotic factors such as type I collagen and fibronectin. TSP1 also initiates phenotypic changes in RTEC with increased expression of α-smooth muscle actin. TSP1 independent of CD47 activates latent transforming growth factor (TGF)-β. These factors are secreted as matrix and lead to fibrosis affecting the renal parenchyma.

deposition, characterized by glomerulosclerosis and tubulointerstitial fibrosis, is the non-specific hallmark of disease progression for which there is no therapeutic intervention. TGF-β is the best known pro-fibrotic cytokine [32], and linked to the development of CKD in numerous pre-clinical [33] and human studies [34] (Fig. 6). In order to bind receptors, TGF-β requires extracellular activation, which can be performed by TSP1 [35, 36]. The role of TSP1 alone in CKD (specifically diabetic nephropathy [14] and glomerulonephritis [15]) has been investigated. We conducted the present study to determine how TSP1-based pathology in CKD is regulated through its high affinity receptor, CD47.

Absent TSP1–CD47 signaling is protective against acute kidney injury (AKI) [9]. Similar to the previously observed effect on CKD resulting from absent TSP1, we also found that targeting CD47 was protective against the development of renal parenchymal fibrosis. Lack of CD47, or treatment with a CD47 blocking antibody reduced pathophysiological fibrosis and expression of fibrotic markers in a model of reduced renal mass (ischemia–reperfusion injury and subsequent nephrectomy, IR-N). $CD47^{-/-}$ mice are robustly protected from ischemia–reperfusion injury [9, 20, 37, 38], therefore the IR-N model potentially lacks equivalence when comparing with (more susceptible) wild-type mice. To counteract the inherent protective effect of absent CD47 expression, we administered αCD47 antibody to WT mice 7 days after the ischemia–reperfusion injury. This antibody is protective in native [9] and transplant-related [16] AKI, and in our study was effective in protecting mice from developing fibrosis. Transcript levels and protein expression of TSP1 were reduced in the IR-N disease model when CD47 signaling was mitigated. TSP1 has been shown to have an effect on fibroblast migration [39] and angiogenesis [40], and this study supports previous work that places TSP1–CD47 signaling central to wound healing [41]. Targeting CD47 to modify progression of fibrosis may be dependent upon both the inherent level of TSP1 in the disease of interest, and therefore the ability of pharmacological intervention to modify signal transduction via TGF-β.

RTEC contribute to the production of matrix proteins, and WT RTEC responded to a hypoxic stimulus by upregulating transcript of fibrotic markers. This effect was muted in $CD47^{-/-}$ cells. A similar pattern of expression was also seen in WT and $CD47^{-/-}$ RTEC in response to exogenous stimulation with TSP1. The effect was recapitulated in human RTEC, and mitigated with CD47 blocking antibody. Incubation with TSP1 induced expression of αSMA, a feature pathognomonic of EMT [42, 43]. RTEC also demonstrate plasticity of phenotype, with features of de-differentiation following injury [44]. Our data clearly show a phenotypic change in response to exposure to TSP1, in addition to elaboration of fibrotic markers. However, the overall contribution of RTEC to fibrosis, in addition to fibroblasts and pericytes [45] has yet to be established. Similarly, inflammatory cells, such as macrophage/dendritic cell subsets contribute to progression of fibrosis (recently reviewed in ref. [46]) and these cells also express TSP1/CD47 [47, 48]. Further studies are required to establish whether these cells are similarly modified by TSP1, and whether the production of matrix protein is altered by limiting signaling through CD47.

It is generally accepted that mouse models are a poor mimic of renal fibrosis; however, we wished to establish whether TSP1 expression is relevant in human CKD. The clinical importance of these results is demonstrated by elevated plasma TSP1 in patients with CKD. TSP1 is normally present at low concentrations in plasma, but increases with vascular damage or inflammation [28, 49]. For the first time, we show significant elevations in plasma TSP1 in patients with CKD, with a continued rise as glomerular filtration rate (GFR) falls. We assessed expression of TSP1 throughout the renal parenchyma to determine whether the increased plasma concentrations of this protein was secreted from the increased fibrotic burden within the kidney. The development of fibrosis alters the distribution of TSP1 expression within renal the parenchyma, but does not markedly increase it. Biopsies from patients with normal renal function show low-level tubular epithelial cell and interstitial expression of TSP1, which becomes more prominent within the fibrosed interstitium, as well as the matrix

of sclerosed glomeruli. There was no substantial difference between the level of TSP1 expression in diabetic versus non-diabetic CKD. The overall level of TSP1 staining in our samples was much less than that seen in a previous study of human diabetic kidney disease [50]. We trialed multiple clones of commercially available TSP1 antibody with similar results, and substantially less background staining. Therefore, it is not yet clear whether the elevation of plasma TSP1 is from the diseased organ, or secondarily affected organs (e.g. the vasculature in CKD).

In summary, we found that matrix protein TSP1 can regulate the production of renal fibrosis markers, and this was attenuated by targeting the high affinity receptor CD47. For the first time, we are able to demonstrate plasma TSP1 as a potential biomarker in CKD. Further studies will enable us to determine whether it provides important prognostic implications for patient outcomes. Finally, the exogenous delivery of CD47 inhibition could offer new therapeutic opportunities in CKD and other pathologies characterized by dysregulated deposition of matrix proteins.

Acknowledgements We have received support from NHMRC Career Development Fellowship (GNT1156977) and project grant (GNT1138372), Sylvia and Charles Viertel Clinical Investigator Grant, Royal Australia College of Physicians Jacquot Establishment Fellowship (all to NMR).

Author contributions NMR initiated and designed the study, conducted experiments, performed data analysis, wrote and approved the manuscript. SJ, BS, NM and KG conducted experiments. BJN provided key biological samples. All authors contributed to editing of the manuscript.

Conflict of interest The authors declare that they have no conflict of interest.

References

1. Jha V, Garcia-Garcia G, Iseki K, Li Z, Naicker S, Plattner B, et al. Chronic kidney disease: global dimension and perspectives. Lancet. 2013;382:260–72.
2. Duffield JS. Cellular and molecular mechanisms in kidney fibrosis. J Clin Invest. 2014;124:2299–306.
3. Chawla LS, Kimmel PL. Acute kidney injury and chronic kidney disease: an integrated clinical syndrome. Kidney Int. 2012;82:516–24.
4. Menshikh A, Scarfe L, Delgado R, Finney C, Zhu Y, Yang H, et al. Capillary rarefaction is more closely associated with CKD progression after cisplatin, rhabdomyolysis, and ischemia-reperfusion-induced AKI than renal fibrosis. Am J Physiol Renal Physiol. 2019;317:F1383–97.
5. Mackensen-Haen S, Bader R, Grund KE, Bohle A. Correlations between renal cortical interstitial fibrosis, atrophy of the proximal tubules and impairment of the glomerular filtration rate. Clin Nephrol. 1981;15:167–71.
6. Bohle A, Christ H, Grund KE, Mackensen S. The role of the interstitium of the renal cortex in renal disease. Contrib Nephrol. 1979;16:109–14.
7. Yang L, Besschetnova TY, Brooks CR, Shah JV, Bonventre JV. Epithelial cell cycle arrest in G2/M mediates kidney fibrosis after injury. Nat Med. 2010;16:535–43.
8. Liu Y. New insights into epithelial-mesenchymal transition in kidney fibrosis. J Am Soc Nephrol. 2010;21:212–22.
9. Rogers NM, Thomson AW, Isenberg JS. Activation of parenchymal CD47 promotes renal ischemia-reperfusion injury. J Am Soc Nephrol. 2012;23:1538–50.
10. Resovi A, Pinessi D, Chiorino G, Taraboletti G. Current understanding of the thrombospondin-1 interactome. Matrix Biol. 2014;37:83–91.
11. Roberts DD, Miller TW, Rogers NM, Yao M, Isenberg JS. The matricellular protein thrombospondin-1 globally regulates cardiovascular function and responses to stress via CD47. Matrix Biol. 2012;31:162–9.
12. Isenberg JS, Ridnour LA, Dimitry J, Frazier WA, Wink DA, Roberts DD. CD47 is necessary for inhibition of nitric oxide-stimulated vascular cell responses by thrombospondin-1. J Biol Chem. 2006;281:26069–80.
13. Wang S, Skorczewski J, Feng X, Mei L, Murphy-Ulrich JE. Glucose up-regulates thrombospondin 1 gene transcription and transforming growth factor-beta activity through antagonism of cGMP-dependent protein kinase repression via upstream stimulatory factor 2. J Biol Chem. 2004;279:34311–22.
14. Daniel C, Schaub K, Amann K, Lawler J, Hugo C. Thrombospondin-1 is an endogenous activator of TGF-beta in experimental diabetic nephropathy in vivo. Diabetes. 2007;56:2982–9.
15. Hochegger K, Knight S, Hugo C, Mayer G, Lawler J, Mayadas TN, et al. Role of thrombospondin-1 in the autologous phase of an accelerated model of anti-glomerular basement membrane glomerulonephritis. Nephron Exp Nephrol. 2004;96:e31–38.
16. Rogers NM, Zhang ZJ, Wang JJ, Thomson AW, Isenberg JS. CD47 regulates renal tubular epithelial cell self-renewal and proliferation following renal ischemia reperfusion. Kidney Int. 2016;90:334–47.
17. Jensen EC. Quantitative analysis of histological staining and fluorescence using ImageJ. Anat Rec. 2013;296:378–81.
18. Yao M, Rogers NM, Csanyi G, Rodriguez AI, Ross MA, St Croix C, et al. Thrombospondin-1 activation of signal-regulatory protein-alpha stimulates reactive oxygen species production and promotes renal ischemia reperfusion injury. J Am Soc Nephrol. 2014;25:1171–86.
19. Maxhimer JB, Shih HB, Isenberg JS, Miller TW, Roberts DD. Thrombospondin-1/CD47 blockade following ischemia-reperfusion injury is tissue protective. Plast Reconstr Surg. 2009;124:1880–9.
20. Isenberg JS, Shiva S, Gladwin M. Thrombospondin-1-CD47 blockade and exogenous nitrite enhance ischemic tissue survival, blood flow and angiogenesis via coupled NO-cGMP pathway activation. Nitric Oxide. 2009;21:52–62.
21. Daniel C, Wiede J, Krutzsch HC, Ribeiro SM, Roberts DD, Murphy-Ulrich JE, et al. Thrombospondin-1 is a major activator of TGF-beta in fibrotic renal disease in the rat in vivo. Kidney Int. 2004;65:459–68.
22. Poczatek MH, Hugo C, Darley-Usmar V, Murphy-Ulrich JA. Glucose stimulation of transforming growth factor-beta bioactivity in mesangial cells is mediated by thrombospondin-1. Am J Pathol. 2000;157:1353–63.

23. Shi-Wen X, Leask A, Abraham D. Regulation and function of connective tissue growth factor/CCN2 in tissue repair, scarring and fibrosis. Cytokine Growth Factor Rev. 2008;19:133–44.
24. Liu Y. Epithelial to mesenchymal transition in renal fibrogenesis: pathologic significance, molecular mechanism, and therapeutic intervention. J Am Soc Nephrol. 2004;15:1–12.
25. Iwano M, Plieth D, Danoff TM, Xue C, Okada H, Neilson EG. Evidence that fibroblasts derive from epithelium during tissue fibrosis. J Clin Invest. 2002;110:341–50.
26. Vongwiwatana A, Tasanarong A, Rayner DC, Melk A, Halloran PF. Epithelial to mesenchymal transition during late deterioration of human kidney transplants: the role of tubular cells in fibrogenesis. Am J Transplant. 2005;5:1367–74.
27. Labrousse-Arias D, Castillo-Gonzalez R, Rogers NM, Torres-Capelli M, Barreira B, Aragones J, et al. HIF-2alpha-mediated induction of pulmonary thrombospondin-1 contributes to hypoxia-driven vascular remodelling and vasoconstriction. Cardiovasc Res. 2016;109:115–30.
28. Kaiser R, Frantz C, Bals R, Wilkens H. The role of circulating thrombospondin-1 in patients with precapillary pulmonary hypertension. Respir Res. 2016;17:96.
29. Smadja DM, d'Audigier C, Bieche I, Evrard S, Mauge L, Dias JV, et al. Thrombospondin-1 is a plasmatic marker of peripheral arterial disease that modulates endothelial progenitor cell angiogenic properties. Arterioscler Thromb Vasc Biol. 2011;31:551–9.
30. Levey AS, Stevens LA, Schmid CH, Zhang YL, Castro AF, Feldman HI, et al. A new equation to estimate glomerular filtration rate. Ann Intern Med. 2009;150:604–12.
31. McClellan AC, Plantinga L, McClellan WM. Epidemiology, geography and chronic kidney disease. Curr Opin Nephrol Hypertens. 2012;21:323–8.
32. Meng XM, Tang PM, Li J, Lan HY. TGF-beta/Smad signaling in renal fibrosis. Front Physiol. 2015;6:82.
33. Becker GJ, Hewitson TD. Animal models of chronic kidney disease: useful but not perfect. Nephrol Dial Transplant. 2013;28:2432–8.
34. Sureshbabu A, Muhsin SA, Choi ME. TGF-beta signaling in the kidney: profibrotic and protective effects. Am J Physiol Renal Physiol. 2016;310:F596–F606.
35. Crawford SE, Stellmach V, Murphy-Ullrich JE, Ribeiro SM, Lawler J, Hynes RO, et al. Thrombospondin-1 is a major activator of TGF-beta1 in vivo. Cell. 1998;93:1159–70.
36. Ribeiro SM, Poczatek M, Schultz-Cherry S, Villain M, Murphy-Ulrich JE. The activation sequence of thrombospondin-1 interacts with the latency-associated peptide to regulate activation of latent transforming growth factor-beta. J Biol Chem. 1999;274:13586–93.
37. Isenberg JS, Hyodo F, Matsumoto K, Romeo MJ, Abu-Asab M, Tsokos M, et al. Thrombospondin-1 limits ischemic tissue survival by inhibiting nitric oxide-mediated vascular smooth muscle relaxation. Blood. 2007;109:1945–52.
38. Isenberg JS, Pappan LK, Romeo MJ, Abu-Asab M, Tsokos M, Wink DA, et al. Blockade of thrombospondin-1-CD47 interactions prevents necrosis of full thickness skin grafts. Ann Surg. 2008;247:180–90.
39. Streit M, Velasco P, Riccardi L, Spencer L, Brown LF, Janes L, et al. Thrombospondin-1 suppresses wound healing and granulation tissue formation in the skin of transgenic mice. EMBO J. 2000;19:3272–82.
40. Soto-Pantoja DR, Shih HB, Maxhimer JB, Cook KL, Ghosh A, Isenberg JS, et al. Thrombospondin-1 and CD47 signaling regulate healing of thermal injury in mice. Matrix Biol. 2014;37:25–34.
41. Agah A, Kyriakides TR, Lawler J, Bornstein P. The lack of thrombospondin-1 (TSP1) dictates the course of wound healing in double-TSP1/TSP2-null mice. Am J Pathol. 2002;161:831–9.
42. Grande MT, Sanchez-Laorden B, Lopez-Blau C, De Frutos CA, Boutet A, Arevalo M, et al. Snail1-induced partial epithelial-to-mesenchymal transition drives renal fibrosis in mice and can be targeted to reverse established disease. Nat Med. 2015;21:989–97.
43. Lovisa S, LeBleu VS, Tampe B, Sugimoto H, Vadnagara K, Carstens JL, et al. Epithelial-to-mesenchymal transition induces cell cycle arrest and parenchymal damage in renal fibrosis. Nat Med. 2015;21:998–1009.
44. Kusaba T, Lalli M, Kramann R, Kobayashi A, Humphreys BD. Differentiated kidney epithelial cells repair injured proximal tubule. Proc Natl Acad Sci USA. 2014;111:1527–32.
45. Humphreys BD, Lin SL, Kobayashi A, Hudson TE, Nowlin BT, Bonventre JV, et al. Fate tracing reveals the pericyte and not epithelial origin of myofibroblasts in kidney fibrosis. Am J Pathol. 2010;176:85–97.
46. Ruiz-Ortega M, Rayego-Mateos S, Lamas S, Ortiz A, Rodrigues-Diez RR. Targeting the progression of chronic kidney disease. Nat Rev Nephrol. 2020;16:269–88.
47. Stein EV, Miller TW, Ivins-O'Keefe K, Kaur S, Roberts DD. Secreted thrombospondin-1 regulates macrophage interleukin-1beta production and activation through CD47. Sci Rep. 2016;6:19684.
48. Braun D, Galibert L, Nakajima T, Saito H, Quang VV, Rubio M, et al. Semimature stage: a checkpoint in a dendritic cell maturation program that allows for functional reversion after signal-regulatory protein-alpha ligation and maturation signals. J Immunol. 2006;177:8550–9.
49. Novelli EM, Kato GJ, Ragni MV, Zhang Y, Hildesheim ME, Nouraie M, et al. Plasma thrombospondin-1 is increased during acute sickle cell vaso-occlusive events and associated with acute chest syndrome, hydroxyurea therapy, and lower hemolytic rates. Am J Hematol. 2012;87:326–30.
50. Hohenstein B, Daniel C, Hausknecht B, Boehmer K, Riess R, Amann KU, et al. Correlation of enhanced thrombospondin-1 expression, TGF-beta signalling and proteinuria in human type-2 diabetic nephropathy. Nephrol Dial Transplant. 2008;23:3880–7.